Optical Materials 96 (2019) 109311

Contents lists available at ScienceDirect

Optical Materials

journal homepage: www.elsevier.com/locate/optmat

Tuning the photoinduced charge transfer from CdTe quantum dots to ZnO nanofilms through Ga doping

Dickson Mwenda Kinyua, Le Niu, Hua Long*, Kai Wang, Bing Wang

Wuhan National Laboratory for Optoelectronics and School of Physics, Huazhong University of Science and Technology, Wuhan, 430074, China

ARTICLE INFO

Keywords:
QDs/ZnO hybrid structures
Doping
Semiconductors
Time-resolve fluorescence spectra
Electron transfer

ABSTRACT

Tuning the charge transfer rate between quantum dots (QDs) and metal oxide (MO) is important for improving the performances of QDs-MO devices. And tailoring the energy band of MO is one way to tune the charge transfer rate. In this work, we enhance the charge transfer rate between CdTe QDs and ZnO through tailoring the optical band gap of ZnO nanofilms by Ga-doping. The Ga doping influenced the photo luminescence (PL) performance of CdTe QDs/ZnO hybrid structures. The results of time-resolved fluorescence spectra revealed that the charge transfer rate from CdTe QDs to ZnO nanofilms could be tuned by varying the Ga doping concentrations in ZnO. And, transfer rate were increased by up to ~4.1 times through Ga doping. In addition, the structure showed electron transfer efficiency improvements to the tune of ~25.3%. We attribute the improvement to efficient electron transfer via band-band transfer and the defects pathways induced by Ga-doping. The experimental results will be useful for improving the efficiency of optical devices using QDs/ZnO hybrid structure.

1. Introduction

Nano-optical devices have important potential applications in many fields [1–4]. Among them, QDs-metal oxide (MO) devices have attracted much attention for their applications in QDs sensitized solar cells [5–7] and QDs emission diodes (QLEDs) [8]. In these devices, electron transfer plays an important role. For example, electron transfer from the light absorbing material (QDs) to the electron collector (MO) enhances the photocurrent, which is crucial in determining the efficiency of solar cells [9,10]. And, to improve the performance of these devices, electron transfer rate should be increased, which is mostly realized by reducing the size of the QDs [11]. This up-shifts conduction band minimum (CBM) of QDs and increases the driving force for electron-transfer to MO [12].

Though the electron transfer rate can be increased by decreasing the QDs size, it also widens bandgap of QDs, which in-turn results in blue shift of the optical-absorption edge. This may result to lower efficiency of the solar cells. Therefore, understanding of the charge transfer mechanisms and tailoring the energy band in QDs/MO devices are critical for optimizing the electron transfer and light harvesting simultaneously. In this work, we propose an optional way to tune electron transfer rate by tailoring the bandgap of the ZnO (MO) nano-films using Ga-dopants, other than by decreasing QDs size.

ZnO is widely used in QD/MO devices because of high electron mobility [13], wide direct band gap [14], and high transparency. And, the performances of ZnO QD/MO devices can be improved by doping [15]. For example, Mg doping in ZnO raises the CBM, thus prevents electron injection from the cathode to QDs, improving QLED performance [16]. Li-doped ZnO nanoparticle photovoltaics has also been reported [17]. Besides, Jung et al. [18] demonstrated that the performance of CdS/CdSe nanocomposite co-sensitized ZnO nanowires device was enhanced by defects and nanoscale strain. However, the effect of Ga doping on charge transfer dynamics in QDs/ZnO hybrid structures has not been reported.

Gallium-doped zinc oxide (GZO) nanostructures are advantageous because close atomic radius; Ga^{3+} (0.062 nm) to Zn^{2+} (0.074 nm) [19,20]. This produces less strain and local lattice distortion in the crystal. Moreover, Ga doping merits because it is less reactive with oxygen [21,22]. Finally, Ga doping increases the transparency of ZnO in the visible region [23]. Here we studied the influences of Ga doping on the photo-induced charge transfer from CdTe QDs to ZnO. The results show that the charge transfer rates and efficiency were tuned through varying Ga doping concentration in ZnO. By using this benefit, we demonstrate how to boost the performance of hybrid structures by slightly doping the MO.

* Corresponding author.
E-mail address: longhua@hust.edu.cn (H. Long).

https://doi.org/10.1016/j.optmat.2019.109311
Received 18 June 2019; Received in revised form 30 July 2019; Accepted 8 August 2019

1.1. Experiment

Ga doped ZnO (GZO) nano-films were fabricated on quartz substrates by pulsed laser deposition with GZO targets of different doping concentrations (0%, 2.9%, 5.0%, and 7.3%) [15]. The GZO targets were sintered at 1350 °C for 48 h in air atmosphere using prescribed amount of ZnO (99.99%) and Ga_2O_3 (99.99%). The Ga contents in the ceramic GZO targets were 2.9%, 5.0% and 7.3%, respectively. The KrF excimer laser beam (Lambda Physik, 248 nm) was focused on the GZO targets through lens. The repetition frequency of the excimer laser was 5 Hz. Before the deposition, the vacuum chamber was evacuated to 4.5×10^{-3} Pa. During the deposition, the oxygen gas pressure was kept at 0.2 Pa. The energy density focused on the GZO target surface was about 2.0 J/cm^2. And, the deposition time was 40 min.

Red and orange CdTe QDs capped by thioglycolic acid were then dispersed on either GZO films or quartz substrates from their diluted aqueous solution via drop casting. Here we marked the orange and red QDs as QD_1 and QD_2, respectively.

The surface morphologies of GZO nanofilms were measured by atomic force microscopy (AFM, Veco NanoScope MultiMode). The UV–visible transmission spectra were measured by a spectrophotometer (HITACHI U3310). Bright field images were obtained using TEM (Tecnai G220, 300 KV) for the as prepared CdTe QDs solution.

The time-resolved photoluminescence (TRPL) measurements were performed using a home-built confocal-microscope configuration and a time-correlated single-photon counting system (Picoquant, PicoHarp 300) [24], pumped by 800 nm fs laser (a mode-locked Ti/Sapphire oscillator, described in details in [25]). The laser beam was focused on hybrid structure by the same 20 × objective (Olympus, NA = 0.4). In addition, the reflected signals was collected using the same objective.

2. Results and discussion

The AFM images of the GZO nanofilm surface with different Ga concentrations are shown in Fig. 1. The grain sizes of the nanofilms decreased with Ga concentration increase due to enhanced nucleation density during doping. This resulted to smoother surface.

Fig. 2(a) shows the plots of $(\alpha h\nu)^2$ versus photon energy ($h\nu$). The inserted figure is the corresponding UV–visible transmission spectra at different Ga concentrations. The optical band gaps (E_g) were obtained using the following formula [26,27]:

$$\alpha h\nu = B(h\nu - E_g)^{1/2} \tag{1}$$

where B is a constant, α is the absorption coefficient. From the figure, we observed that E_g increased from 3.24 to 3.49 eV with Ga concentrations increase, which was attributed to the Burstein-Moss effect [28]. Fig. 2(b and c) shows the transmission electron microscope images of QD_1 and QD_2 respectively. The diameter of the QDs was estimated to be about 3.5 nm and 3.8 nm respectively. The inserted Fig. 2(b and c) show the images of QDs solutions.

The absorption and PL spectra of CdTe QDs solutions are shown in Fig. 3(a). The emission peaks were at 605 nm and 635 nm for QD_1 and QD_2, respectively. Fig. 3(b) shows PL spectra of QD_1 on quartz and GZO nano-films. From the figure, it is clear that the emission intensity of QDs was reduced with the introduction of Ga dopants in ZnO. The quenching effect was attributed to deactivation of excitons via electron transfer to GZO at QD/GZO interfaces and/or intra-gap assisted non-radioactive recombination [29]. The QD_2 on GZO nano-films also showed similar behavior.

Fig. 4 (a, b) shows the decay results of the time resolved PL emission (pumped at 800 nm) from QD_1 and QD_2 on GZO nanofilms, respectively. The experimental results can be fitted using a biexponential decay function:

$$I = \alpha_1 \times \exp\left(-\frac{t}{\tau_1}\right) + \alpha_2 \times \exp\left(-\frac{t}{\tau_2}\right) \tag{2}$$

where I is the PL intensity, α_1 and α_2 are pre-exponential factors, τ_1 and τ_2 are corresponding fast and slow lifetime, respectively. Additionally, we determined the average emission lifetimes ($\bar{\tau}$) [30]:

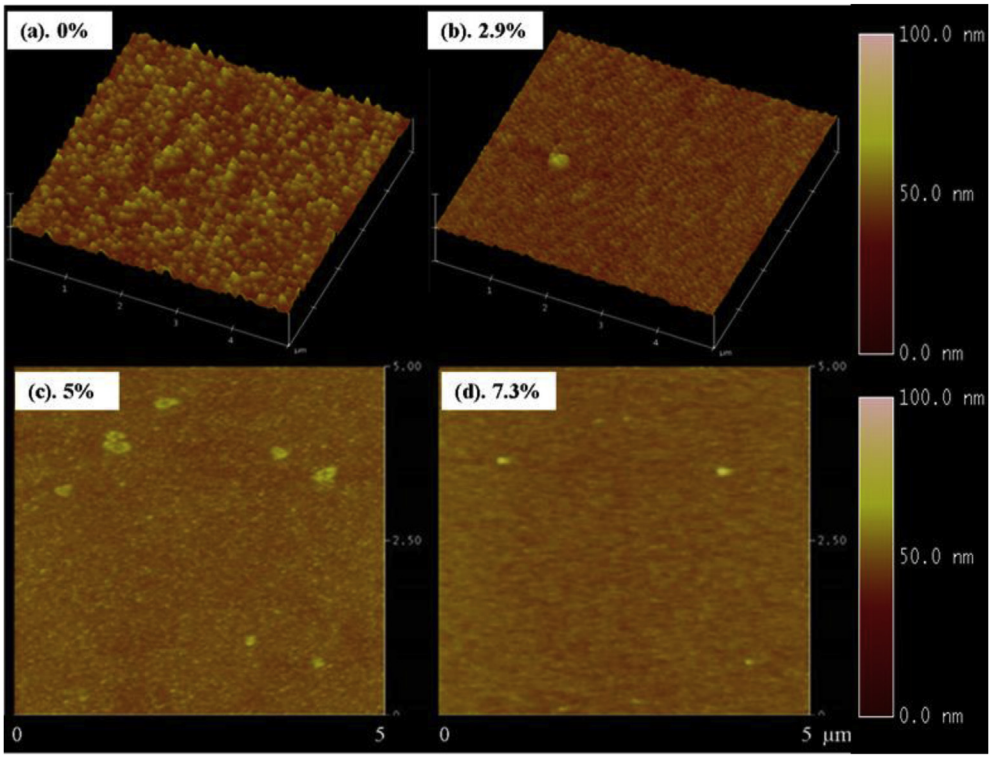

Fig. 1. AFM images of GZO nano-films with different Ga concentration. (a, b) shows the 3-D micrograph which reveals reduction in surface roughness and enhanced smoothening of the surface [see (c, d)] due to reduction in grain size.

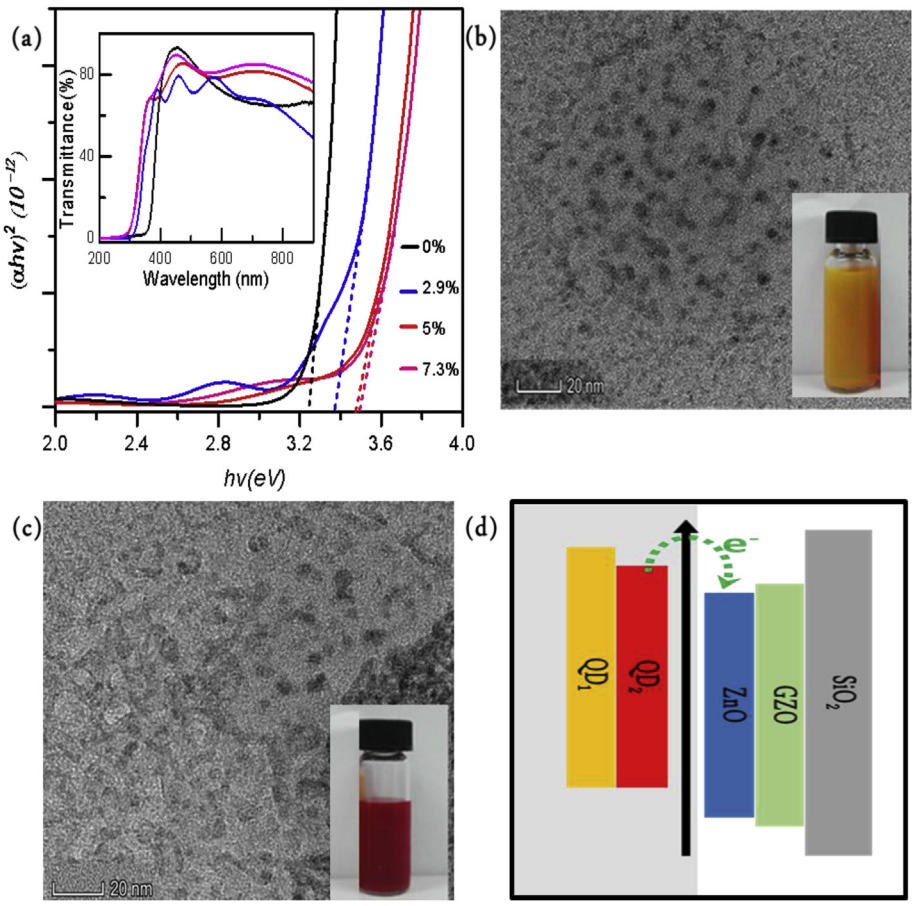

Fig. 2. (a) The plots of $(ahv)^2$ versus energy (hv) for GZO films with different Ga concentrations. The inserted figure is the corresponding UV–visible transmission spectra. (b, c) shows the TEM images of QD_1 and QD_2 respectively. The inserted figures (b, c) show QDs solution image. (d) Scheme of the relative energy differences between CdTe (donor) and MO (acceptor) of the hybrid structure.

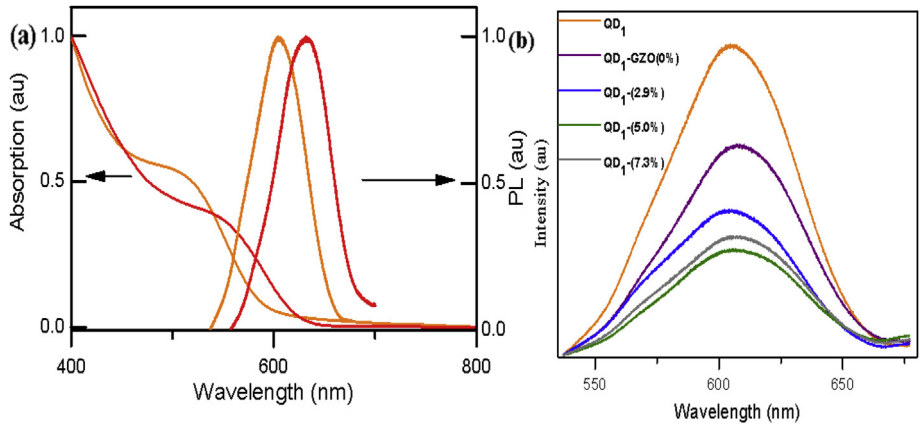

Fig. 3. (a) Absorption and emission spectra of QD1 and QD2 solutions. (b) The PL spectra of the QD1/GZO hybrid structures with different Ga doping concentration.

$$\overline{\tau} = \frac{\alpha_1\tau_1^2 + \alpha_2\tau_2^2}{\alpha_1\tau_1 + \alpha_2\tau_2} \quad (3)$$

The fitted decay lifetime values were shown in Table 1. The short lifetimes (τ_1) were related to a convolution of trapping and non-radioactive energy transfer. The long decay lifetime (τ_2) of QDs on quartz (SiO_2) is related to electron-hole radioactive recombination, whereas the τ_2 of QDs coupled on GZO is attributed to a combination of electron-hole radiative recombination and back electron transfer at the QD/MO interface. τ_2 continuously reduces as the Ga contents were increased which could be attributed to enhanced charge transfer activities.

As shown in Table 1, $\overline{\tau}$ of QDs on GZO decreased compared to QDs on undoped ZnO, suggesting an apparent increase of the electron transfer rate from QDs to GZO nanofilms. This result implies that the electron transfer can be manipulated by Ga doping. We then calculated the charge transfer rate constant (K_{et}) for the QDs/ZnO hybrid structure using equation (4) [31]. To deconvolute electron transfer as a result of Ga doping, we make the assumption that the only difference between the kinetic behavior of an electron-hole pair in a QD coupled to SiO_2 and one coupled to GZO is the added pathway of electron transfer. Under this assumption, the electron transfer rate can be calculated as follows:

$$K_{et} = \frac{1}{\overline{\tau}_{QDs+GZO}} - \frac{1}{\tau_{QDs}} \quad (4)$$

where $\overline{\tau}_{QDs+GZO}$ is the average lifetime of QDs on GZO, while τ_{QDs} is lifetime of the QDs on quartz. When QD_1 and QD_2 were coupled to GZO nanofilms, the k_{et} show enhancement factor as high as ~4.1 and ~2.7,

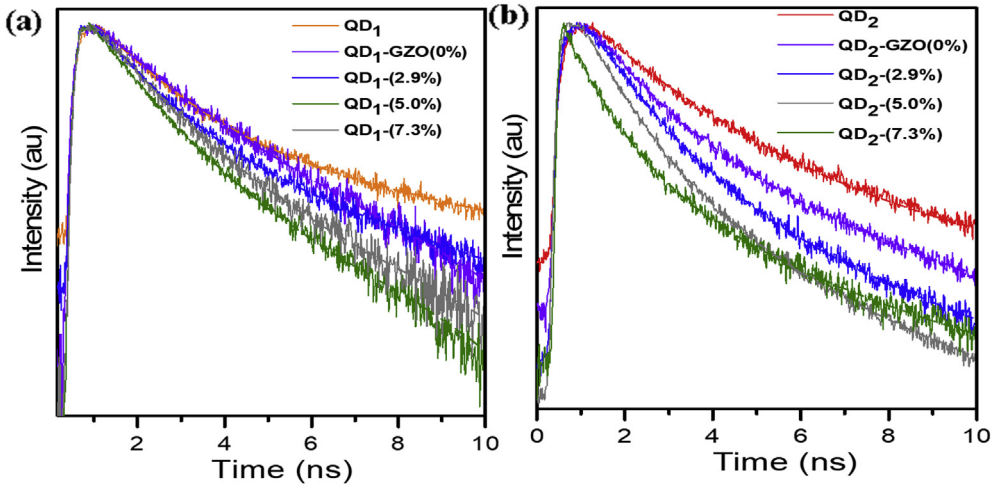

Fig. 4. Time resolved PL results of QD_1/GZO (a) and QD_2/GZO (b) hybrid structures. The dotted lines show the fitting curves using biexponential decay function.

Table 1
The PL decay lifetimes of QD_1 and QD_2 on quarts and GZO nano-films.

Sample	α_1	τ_1 (ns)	α_2	τ_2 (ns)	$\bar{\tau}$ (ns)	$K_{et} \times 10^8$ (s^{-1})
QD_1	0.14	0.8708	0.86	3.0042	2.9008	
QD_1-GZO (0%)	0.15	0.8400	0.85	2.7831	2.6848	0.2775
QD_1-GZO (2.9%)	0.38	0.9317	0.62	2.6524	2.3684	0.7749
QD_1-GZO (5.0%)	0.45	0.8267	0.55	2.5185	2.1603	1.1817
QD_1-GZO (7.3%)	0.31	0.7412	0.69	2.5110	2.3038	0.8933
QD_2	0.06	0.944	0.93	3.4962	3.4525	
QD_2-GZO (0%)	0.13	0.8926	0.87	3.2621	3.1690	0.2591
QD_2-GZO (2.9%)	0.33	1.0581	0.67	3.2826	2.9778	0.4617
QD_2-GZO (5.0%)	0.49	1.1683	0.51	3.2551	2.7200	0.7800
QD_2-GZO (7.3%)	0.42	0.8012	0.58	3.3499	2.9546	0.4881

respectively (see Fig. 5(a) on the influences of Ga doping). Furthermore, the k_{et} of QD_1 was larger than that of QD_2, which was attributed to the quantum confinement effect [32] and conduction band shifting to more negative with QDs size decrease [30]. The k_{et} increased with the increasing band gap energy difference between the donor (QDs) and acceptor (ZnO). However, further increase Ga concentration to 7.3% will induce decrease of K_{et}, which can be attributed to the high density of states and reduced band gap at high doping concentration [33].

Generally, fast electron transfer reduces electron-hole recombination [34] and more electrons could be injected to ZnO, leading to improved performance of QDs/ZnO structure. According to Marcus model [35], K_{et} is dependent on the band difference gradient between the QDs and MO. Ga-doping leads to upshift of the CBM of ZnO (see Fig. 2 (d)), which reduces this band energy gradient. Nevertheless, other factors can also influence the K_{et}. For example, Fahimi et al. showed ZnO had a higher K_{et} than TiO_2 despite the fact that the CBM of ZnO is higher than that of TiO_2, which was attributed to high electronic coupling matrix element in ZnO compared to TiO_2 [9]. Moreover, Ga doping enhances energy defects [36,37] which could act as a passageway to facilitate electron transfer [17]. Ding et al. [38], reported high electron transfer efficiency using Mg doped ZnO despite the fact that Mg upshifted the CBM of ZnO. They attributed this to enhanced defects, which served as alternative pathways for electron transfer. Finally, we calculate the electron transfer efficiency (η_{ET}) as a result of Ga doping using equation (5) [39]:

$$\eta_{ET} = 1 - \frac{\bar{\tau}_{QD+GZO}}{\tau_{QD}} \tag{5}$$

The calculated charge transfer efficiencies are 7.7%, 18%, 25.3% and 20.8% for 0%, 2.9%, 5% and 7.3% Ga doped ZnO sensitized with QD_1 respectively. While charge transfer efficiencies using QD_2 are 8.3%, 13.8%, 21.2% and 14.4% for 0%, 2.9%, 5% and 7.3% respectively. This gradual increase in the efficiency as the Ga doping concentration increases (see Fig. 5 (b)), suggests that the indeed charge transfer can still be enhanced through the defects induced by doping.

3. Conclusions

The electron transfer characteristics of CdTe QDs coupled to GZO nano-films were studied. The results systematically demonstrated that the hybrid structure can enhance electron transfer rate and efficiency through additional pathways (defect states) induced by Ga doping.

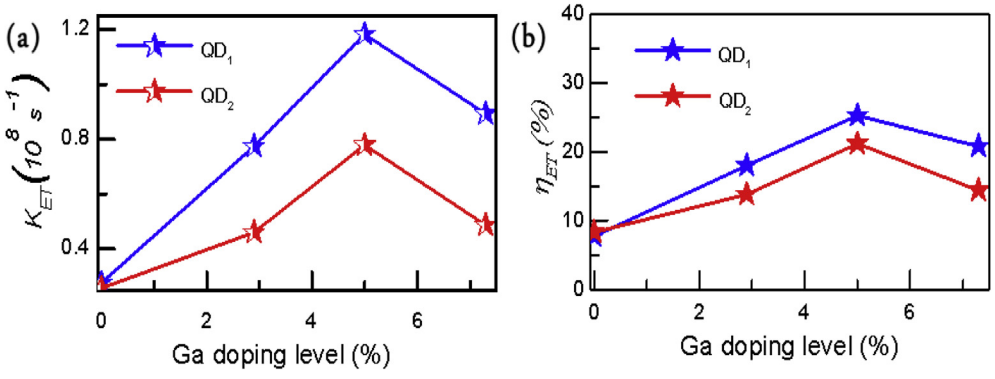

Figure 5. (a, b) shows the influence of Ga doping on the electron transfer rate and efficiency(η_{ET}) respectively.

Besides, these results show the possibility of tuning the K_{et} in CdTe QDs/ZnO hybrid structure through Ga doping. The increased K_{et} can lead to a reduction in electron-hole recombination, which can be helpful to improve the performance of QDs/MO devices.

Conflicts of interest

The authors declare that they have no known conflicts of interest.

Acknowledgment

This work was supported by the National Natural Science Foundation of China (nos. 11774115, 91850113), the 973 Programs under grants 2014CB921301, and the Doctoral Fund of Ministry of Education of China under Grant No. 20130142110078.

References

[1] S.K. Shrama, N. Saurakhiya, S. Barthwal, R. Kumar, A. Sharma, Nanoscale Res. Lett. 9 (2014) 122.
[2] H. Chen, C. Qin, B. Wang, P. Lu, Opt. Lett. 44 (2019) 363–366.
[3] M. Willander, L.L. Yang, A. Wadeasa, S.U. Ali, M.H. Asif, Q.X. Zhao, O. Nur, J. Mater. Chem. 19 (2009) 1006–1018.
[4] D. Zhao, S. Ke, Y. Hu, B. Wang, P. Lu, J. Opt. Soc. Am. B 36 (2019) 1731–1737.
[5] J. Chen, J. Song, X. Sun, W. Deng, C. Jiang, W. Lei, J. Huang, R. Liu, Appl. Phys. Lett. 94 (2009) 153115.
[6] Y. Wang, Z. Yang, Y.X. Huang, Y.X. Yan, J. Hou, Z.M. Li, G.Z. Cao, ACS Appl. Energy Mater. 2 (2019) 1259–1265.
[7] Z.X. Pan, H.S. Rao, I. Mora-Sero, J. Bisquert, X.H. Zhong, Chem. Soc. Rev. 47 (2018) 7659–7702.
[8] D.V. Talapin, J.-S. Lee, M.V. Kovalenko, E.V. Shevchenko, Chem. Rev. 110 (2009) 389–458.
[9] M.J. Fahimi, D. Fathi, M. Ansari-Rad, Phys. E Low-dimens. Syst. Nanostruct. 73 (2015) 148–155.
[10] Y.L. Chen, Y.H. Chen, J.W. Chen, F.R. Cao, L. Li, Z.M. Luo, I.C. Leu, Y.C. Pu, ACS Appl. Mater. Interfaces 11 (2019) 8126–8137.
[11] J. Xu, Z. Chen, J.A. Zapien, C.S. Lee, W. Zhang, Adv. Mater. 26 (2014) 5337–5367.
[12] K. Zidek, K.B. Zheng, C.S. Ponseca, M.E. Messing, L.R. Wallenberg, P. Chabera, M. Abdellah, V. Sundstrom, T. Pullerits, J. Am. Chem. Soc. 134 (2012) 12110–12117.
[13] Ü. Özgür, Y.I. Alivov, C. Liu, A. Teke, M. Reshchikov, S. Doğan, V. Avrutin, S.-J. Cho, H. Morkoc, J. Appl. Phys. 98 (2005) 11.
[14] X. Han, K. Wang, H. Long, H. Hu, J. Chen, B. Wang, P. Lu, ACS Photonics 3 (2016) 1308–1314.
[15] A.A. Habeeb, H. Long, L. Bao, K. Wang, B. Wang, P. Lu, Mater. Lett. 172 (2016) 36–39.
[16] Y. Sun, Y. Jiang, H. Peng, J. Wei, S. Zhang, S. Chen, Nanoscale 9 (2017) 8962–8969.
[17] W.H. Cheng, J.W. Chiou, M.Y. Tsai, J.S. Jeng, J.S. Chen, S.L.C. Hsu, W.Y. Chou, J. Phys. Chem. C 120 (2016) 15035–15041.
[18] K. Jung, J. Lee, Y.M. Kim, J. Kim, C.U. Kim, M.J. Lee, Electrochim. Acta 220 (2016) 500–510.
[19] V. Assuncao, E. Fortunato, A. Marques, A. Goncalves, I. Ferreira, H. Aguas, R. Martins, Thin Solid Films 442 (2003) 102–106.
[20] G.K. Paul, S.K. Sen, Mater. Lett. 57 (2002) 742–746.
[21] E. Fortunato, L. Raniero, L. Silva, A. Goncalves, A. Pimentel, P. Barquinha, H. Aguas, L. Pereira, G. Goncalves, I. Ferreira, Sol. Energy Mater. Sol. Cells 92 (2008) 1605–1610.
[22] D.M. Kinyua, H. Long, X. Xing, S. Njoroge, K. Wang, B. Wang, P. Lu, Nanotechnology 30 (2019) 305201.
[23] Y.-D. Ko, K.-C. Kim, Y.-S. Kim, Superlattice Microstruct. 51 (2012) 933–941.
[24] X. Li, W. Liu, Y. Song, C. Zhang, H. Long, K. Wang, B. Wang, P. Lu, 7 (2019) 1801270.
[25] N.M. Jassim, K. Wang, X. Han, H. Long, B. Wang, P. Lu, Opt. Mater. 64 (2017) 257–261.
[26] N. Serpone, D. Lawless, R. Khairutdinov, J. Phys. Chem. 99 (1995) 16646–16654.
[27] H. Long, L. Bao, K. Wang, S. Liu, B. Wang, Opt. Mater. 60 (2016) 571–576.
[28] M.-C. Jun, S.-U. Park, J.-H. Koh, Nanoscale Res. Lett. 7 (2012) 639.
[29] Y. Sun, Y. Jiang, H. Peng, J. Wei, S. Zhang, S. Chen, Nanoscale 9 (2017) 8962–8969.
[30] A. Kongkanand, K. Tvrdy, K. Takechi, M. Kuno, P.V. Kamat, J. Am. Chem. Soc. 130 (2008) 4007–4015.
[31] H.-M. Cheng, K.-Y. Huang, K.-M. Lee, P. Yu, S.-C. Lin, J.-H. Huang, C.-G. Wu, J. Tang, Phys. Chem. Chem. Phys. 14 (2012) 13539–13548.
[32] A. Shi, J. Sun, Q. Zeng, C. Shao, Z. Sun, H. Li, X. Kong, J. Zhao, J. Lumin. 131 (2011) 1536–1540.
[33] F. Chaabouni, B. Khalfallah, M. Abaab, Thin Solid Films 617 (2016) 95–102.
[34] X.W. Sun, J. Chen, J.L. Song, D.W. Zhao, W.Q. Deng, W. Lei, Opt. Express 18 (2010) 1296–1301.
[35] K. Tvrdy, P.A. Frantsuzov, P.V. Kamat, Proc. Natl. Acad. Sci. 108 (2011) 29–34.
[36] Y. Zou, H. Yang, H. Wang, D. Lou, C. Tu, Y. Zhang, Phys. B Condens. Matter 414 (2013) 7–11.
[37] S.J. Guan, L. Yamawaki, P. Zhang, X.W. Zhao, Top. Catal. 61 (2018) 1585–1590.
[38] C. Ding, Y. Zhang, F. Liu, Y. Kitabatake, S. Hayase, T. Toyoda, R. Wang, K. Yoshino, T. Minemoto, Q. Shen, Nanoscale Horiz. 3 (2018) 417–429.
[39] M. Sun, D. Zhu, W. Ji, P. Jing, X. Wang, W. Xiang, J. Zhao, ACS Appl. Mater. Interfaces 5 (2013) 12681–12688.